J. Phys. A: Math. Gen. 27 (1994) 55–77. Printed in the UK

Scaling properties of a scattering system with an incomplete horseshoe

B Rückerl and C Jung
Fachbereich Physik, Universität Bremen, 2800 Bremen, Federal Republic of Germany

Received 3 June 1993, in final form 15 September 1993

Abstract. We investigate a parameter-dependent map describing a chaotic scattering system. In parameter ranges leading to an incomplete horseshoe we construct an approximate symbolic dynamics which describes quite well the hyperbolic component of the invariant set. Its grammatical rules are correlated with the convergence properties of the thermodynamical formalism for the measures characterizing the invariant set.

1. Introduction

It has always been the task of scattering theory to find out, how properties of a system can be extracted from asymptotic measurements on the projectile, in particular from the deflection function, the time-delay function or similar objects. In the case of chaotic scattering (for reviews see [1, 2]) these functions contain singularities on a fractal subset of their domain. Scattering chaos of this type has been found in a large variety of systems, e.g. in classical models for molecular reactions (for these processes see the review [3]), in model computations for satellite encounters [4], for vortex scattering in hydrodynamics [5], in soliton scattering [6], for particle transport in an open hydrodynamical flow [7] and for various models of potential scattering. Therefore, any improvement in our understanding of chaotic scattering and in particular any enlargement of our methods to attack such systems has the chance to be useful in a wide variety of physical subfields.

In the case of chaos and its associated fractal structures we must find out how we extract from these structures quantities which characterize the complicated motion inside the interaction region. Chaotic scattering is the Hamiltonian version of transient chaos [8]. The skeleton of all complicated motion is a chaotic invariant set (the chaotic saddle) in the phase space. In its vicinity scattering trajectories are kept for a while and trace out temporarily the type of motion performed permanently by the localized chaotic trajectories. The chaotic set has a relatively simple structure only when it is completely hyperbolic. For an example of a complete description of the invariant set in such a case see [9]. In the completely hyperbolic case the invariant set consists of unstable periodic orbits (which are all hyperbolic in this case) and their homoclinic and heteroclinic connections only, it does not contain KAM tori, cantori or any subsets of marginal stability. It is a pure example of the type of invariant set occuring in Smale's horseshoe construction [10]. Its fractal structure and the measures characterizing it as e.g. dimension, entropy, Lyapunov exponents, escape rate, etc can be extracted from scattering data, in particular from the arrangement of the singularities in the deflection function or the time delay function. The appropriate method to do this is the thermodynamical formalism [11, 12]. In the non-hyperbolic case the invariant set contains KAM surfaces and cantori around them in addition. They are more sticky than

0305-4470/94/010055+23$07.50

purely hyperbolic sets [13–15] and make a complete description of the invariant set very complicated.

Fortunately, in most cases the non-hyperbolic influences become noticable only on the long-time behaviour and on very fine resolution. Many properties of the system and its behaviour on short time-scales are dominated by the hyperbolic component of the invariant set. Therefore it is worth while to find ways to extract the properties of this component from scattering functions.

In this paper we shall investigate such possibilities. For simplicity we take an iterated map describing the unbound motion of a kicked particle in a one-dimensional position space. The map contains one free parameter such that the system is completely hyperbolic for large parameter values and pruning sets in below a threshold value of this parameter. For a few examples of a symbolic dynamic with pruning for an open system see [16–18]. For some general considerations of pruned symbolic dynamics and their evaluation see [19, 20].

Our model and its parameter dependence will be presented in section 2. We investigate the homoclinic tangle of the most important unstable fixed point and derive from it possibilities for an approximate symbolic dynamics, first for one particular small range of parameter values. In section 3 we compare the structure of the homoclinic tangle with the structure of singularities in the time-delay function. Section 4 shows the limitations of the approximate symbolic dynamics. In section 5 we can use our knowledge to understand the convergence properties of the thermodynamical formalism for the extraction of measures of the hyperbolic component of the invariant set. Section 6 shows how these ideas can be realized for more general parameter ranges and section 7 contains concluding remarks.

2. The model and its parameter dependence

We describe the motion of a kicked particle on the one-dimensional line by the iterated map P

$$q(n+1) = q(n) + p(n) \qquad p(n+1) = p(n) + Af(q(n+1)) . \tag{1}$$

Here q is the position coordinate, p is the momentum coordinate, n is the discrete time, and A is a free parameter. For the force function we take the particular function

$$f(q) = q(q-1)\exp(-q) . \tag{2}$$

The phase space is the q, p-plane. By a simple transformation the map can be cast into the form

$$\tilde{q}(n+1) = \tilde{q}(n) + T\tilde{p}(n) \qquad \tilde{p}(n+1) = \tilde{p}(n) + f(\tilde{q}(n+1)) \tag{3}$$

where now the free parameter T is the time between two consecutive kicks. We found it more convenient to work with the form (1).

The force given in (2) corresponds to the potential

$$V(q) = \int_q^\infty \mathrm{d}s\, s(s-1)\exp(-s) = (q^2+q+1)\exp(-q) . \tag{4}$$

Our motivation to choose a map of this kind is two-fold. First, we are interested in a parameter dependent smooth map in contrast to the non-smooth systems investigated

in [16–18]. Accordingly, in our system homoclinic/heteroclinic bifurcations are generic tangencies, whereas in non-smooth maps a corner of one manifold hits another manifold. Thereby we hope to obtain the generic, structurally stable scenario. Second, the potential (4) has the structure of a radial potential with centrifugal barrier similar to potentials occuring in atomic scattering processes.

The potential (4) has a minimum at $q = 0$ and a relative maximum at $q = 1$. The maximum leads to the fixed point

$$x_0 = (q_0, p_0) = (1, 0) \tag{5}$$

of the equations of motion (1) and the minimum of the potential leads to the fixed point

$$x_1 = (q_1, p_1) = (0, 0)\,. \tag{6}$$

The point x_0 is always an unstable hyperbolic point. The eigenvalues of the Jacobi matrix of P at x_0 depend on A and are given by

$$\lambda_{1,2} = 1 + A/2e \pm (A/e + A^2/4e^2)^{1/2}\,. \tag{7}$$

At the point x_1 the eigenvalues of the Jacobi matrix of P are

$$\mu_{1,2} = 1 - A/2 \pm (-A + A^2/4)^{1/2}\,. \tag{8}$$

The point x_1 turns from elliptic to inverse hyperbolic at $A = 4$.

At $A = 0$ the system is completely integrable, while for $A \neq 0$ we find transverse homoclinic intersections of the invariant manifolds of x_0. Accordingly for $A \neq 0$ the map P contains topological chaos. For $A > A_1 \approx 5.5$ the system is completely hyperbolic. Then it has a complete Smale horseshoe and can be described by a binary symbolic dynamics without any pruning and therefore with trivial grammatical rules. For $A < A_1$ pruning sets in, the horseshoe becomes incomplete and we find a mixed phase space having KAM tori.

Fortunately, the KAM tori do not have a large influence on the scattering behaviour and therefore let us try to describe the hyperbolic part of the invariant set. For some parameter values this can be done in a rather complete way. The motivation for the choice of the appropriate parameter intervals comes from the plot of the topological entropy K_0, or of the corresponding branching ratio $B = \exp(K_0)$, of the invariant set. Let us first present some results, for it is more convenient to explain later how these results have been obtained in detail. Figure 1 shows a plot of B versus A. Most striking are the steps in this function in which B changes only slowly. We have the impression that there are intervals in which no important bifurcations occur and in which the grammatical rules for the symbolic dynamics to be constructed do not change drastically. A few of this steps in the figure are labelled by a number α whose meaning will become clear later.

The most prominent step is the interval $I_{1/2} = (A_{1/2-}, A_{1/2+})$ (labelled by $\frac{1}{2}$ in the figure). The nature of the relative stability of the dynamics inside this interval and the absence of important bifurcations can be understood from a plot of the invariant manifolds of x_0 as presented in figure 2. All homoclinic intersections and also all other points of the invariant set are contained in the curvilinear rectangle R with the corners x_0, y_1, y_2, y_3. Most important is the observation that the tips of the tendrils of the manifolds reach into empty space, i.e. into gaps which are free of manifolds. Therefore a small stretching or compression of the tendrils does not produce homoclinic tangencies. Now we have to realize that a change of A has the effect on the manifolds that they change their length and

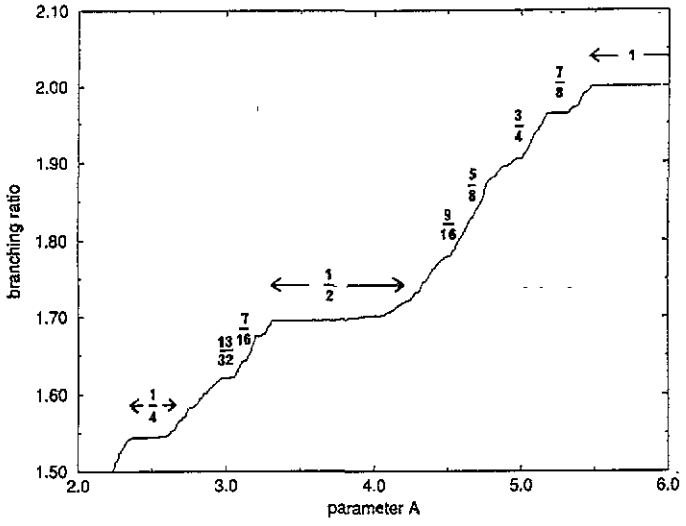

Figure 1. Branching ratio B versus parameter A computed from the number of intervals of the various levels in the time-delay function. A few of the intervals I_α are indicated and labelled by α.

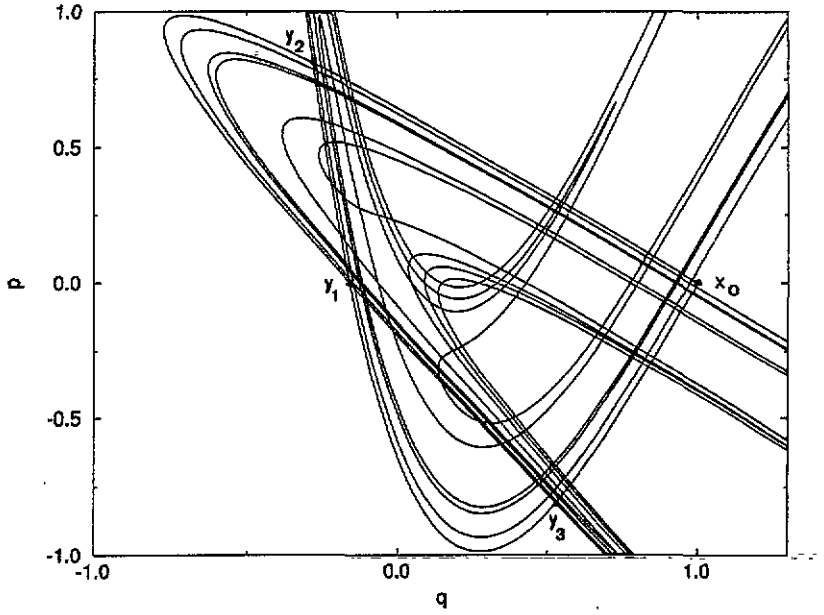

Figure 2. Numerical construction of the invariant manifolds of the fixed point x_0 for the parameter value $A = 3.4$, which lies inside $I_{1/2}$ but close to its lower end. All tendrils up to level 4 are plotted.

can produce homoclinic bifurcations whenever the tip of a tendril hits another manifold. However, when the tips reach into areas free of other manifolds then a small change of the length avoids tangencies and homoclinic bifurcations at least in some small interval of

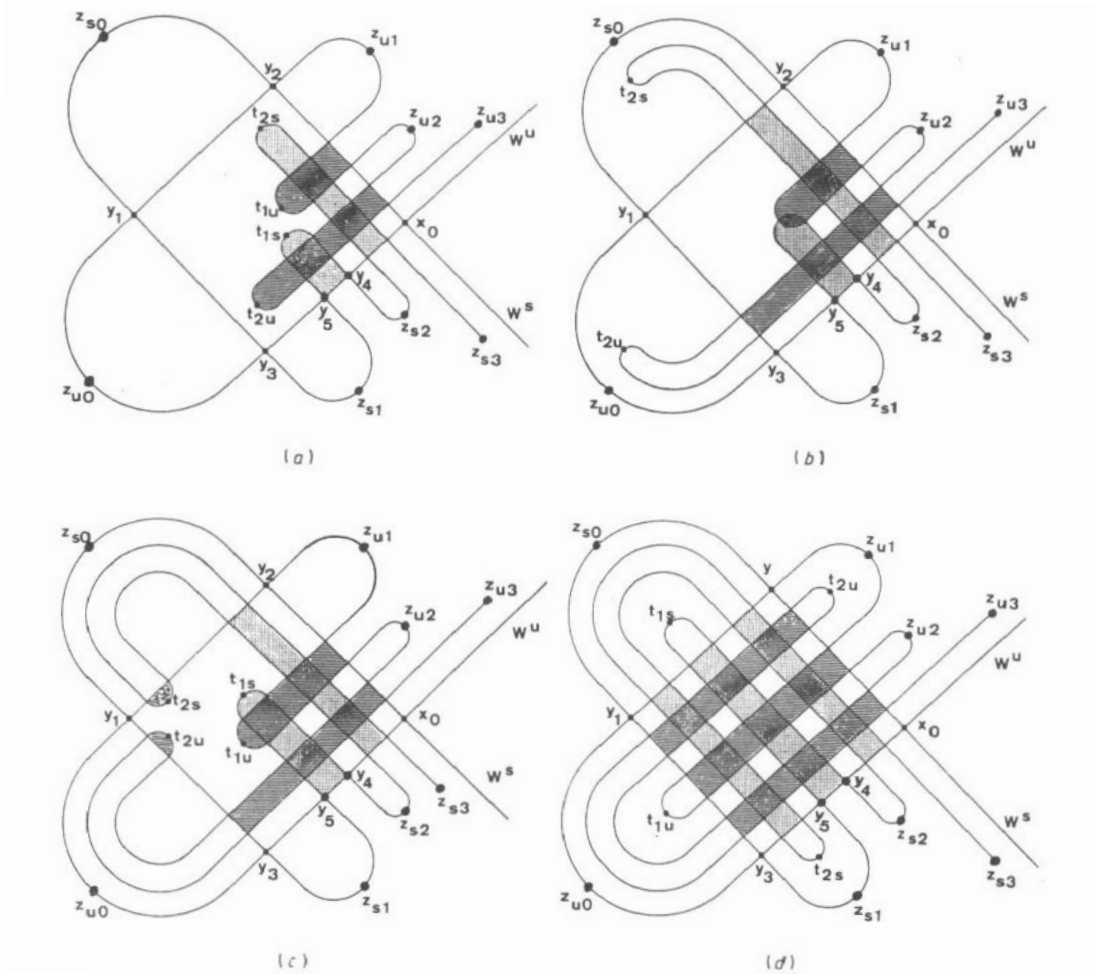

Figure 3. Schematic plot of the tendrils of the invariant manifolds of x_0. Tendrils up to level 2 are included. Part (*a*) shows the situation for $A < A_{1/2-}$, part (*b*) shows the situation for $A_{1/2-} < A < A_{1/2+}$, part (*c*) shows the situation for $A > A_{1/2+}$, part (*d*) shows the case of a complete horseshoe for $A > A_1$. The hatched areas indicate gaps inside tendrils of W^u which are free of higher level tendrils of W^u. The dotted areas indicate gaps inside tendrils of W^s which are free of higher level tendrils of W^s.

values of A. This is exactly what happens in the interval $I_{1/2}$ and in other intervals of slow change of K_0. In these particular intervals we hope to avoid many of the problems which occur generally in wild hyperbolic sets as described in section 6.7 of [21].

Let us explain this effect in detail with the aid of a schematic plot, figure 3. For A just below $A_{1/2-}$ we have a situation for the stable and unstable manifolds W^s and W^u of x_0 as shown in figure 3(*a*). Also here all homoclinic intersections are located inside the rectangle R with the corners x_0, y_1, y_2, y_3. The tendrils of the hierarchy levels 1 and 2 are plotted as the labels on the tips of the tendrils indicate. The tip of the tendril of level m is labelled by $t_{m,u}$ or $t_{m,s}$ for the unstable and the stable manifold respectively. $t_{m+1,u}$ is the image of $t_{m,u}$ under P and $t_{m+1,s}$ is the pre-image of $t_{m,s}$ under P. The hatched areas are gaps inside

tendrils of W^u and these areas are void of further tendrils of W^u coming from higher levels in the hierarchy. All higher level tendrils of W^u are contained in the unhatched areas. In the same way the dotted areas mark the gaps inside tendrils of W^s and these areas are void of further tendrils of W^s coming from higher levels. Therefore in the situation as shown in figure 3(a) the tips of the tendrils will in general undergo homoclinic tangencies when their length is varied during a small change of A.

Next, let A increase somewhat such that a situation like the one in figure 3(b) is created. Now the tips of the tendrils (the ones of higher levels not plotted in the figure as well as the ones shown in figure 3(b)) are either outside of R (as the ones of level 2) or lie in the hatched area (as the ones of level 1). When the tips of two tendrils intersect each other in 2 points (as the tips of the tendrils of level 1 do) then we count this also as a situation in which the tip of one tendril lies inside the interior of the other tendril. We have to take a point in the small arc lying in the hatched/dotted area as the true tip. Therefore small changes of their length (small changes of A) do not cause homoclinic bifurcations. We have a situation with $A \in I_{1/2}$. If A becomes larger than $A_{1/2+}$, then we find a situation like the one in figure 3(c). Now the tips of the tendrils lie outside of the gaps again and accordingly they can again create homoclinic tangencies at small variations of A. For comparison figure 3(d) shows the situation for A just above A_1. Here all tips of tendrils lie outside of R.

With the aid of figure 3 we can also explain more precisely how we divide the invariant manifolds into the various tendrils. First we mark points $z_{u,m}$ on W^u and $z_{s,m}$ on W^s such that one of those points lies on each arc of the invariant manifolds which lies outside of the fundamental rectangle R. The first one has index 0 the other ones have as indices the natural numbers according to their order along the manifolds. It is natural to make the choice such that $z_{u,m+1}$ is the image of $z_{u,m}$ under P and $z_{s,m+1}$ is the pre-image of $z_{s,m}$. By $L_{u,m}$ or $L_{s,m}$ we denote the arcs between $z_{u,m}$ and $z_{u,m+1}$ or between $z_{s,m}$ and $z_{s,m+1}$ respectively. The local arc of W^u, i.e. the one from x_0 to $z_{u,0}$, we denote by $L_{u,-}$, in the same way the local arc of W^s, i.e. the one from x_0 to $z_{s,0}$ is denoted by $L_{s,-}$. $L_{u,m}$ is the image of $L_{u,0}$ under P^m and $L_{s,m}$ is the image of $L_{s,0}$ under P^{-m}. When we speak of the tendril of level m in the following we mean the arc $L_{u,m}$ or $L_{s,m}$ respectively or the parts of them which lie inside R.

The value of the parameter α is determined as follows. α has the value $r2^{-k}$ if the tip of the tendril of level 1 lies inside that gap of level k which is the rth of all gaps of level k, where we count them as follows. Consider all the gaps of W^u (for W^s everything goes symmetrically) in the complete horseshoe construction as shown in figure 3(d). There are 2^{k-1} ones created by the tendril of level k. Count them with only the odd numbers (to avoid cancellations between numerator and denominator in α) from 1 to $2^k - 1$ in the order in which they intersect the arc (x_0, y_2) of W^s, i.e. give the number 1 to the gap lying closest to x_0, the number 3 to the next one, etc and the number $2^k - 1$ to the one lying closest to y_2. For lower values of A all the gaps which remain keep the same number as in the complete case, even though for $A < A_1$ some gaps in between have disappeared. A comparison of the schematic plots of figures 3(b), 3(d), 10(a), 10(b), 13, where the values of α are $\frac{1}{2}$, 1, $\frac{1}{4}$, $\frac{3}{4}$ and $\frac{3}{8}$ respectively, may help to get a feeling for this definition of α.

For these rules we have only taken into account the primary tendrils as shown in figure 3. We have disregarded the secondary tendrils as they will be described in section 4.

3. The time-delay function and its hierarchical organization

Now we are in the position to explain the construction of the time-delay function: a scattering trajectory has the time-delay $Dt = n$, if n of its points lie inside of R. To

construct the time-delay function we have first to give a scheme of how to label asymptotes of scattering trajectories. In the asymptotic region (i.e. in the region $q \to +\infty$) the force converges to zero rapidly, so that the asymptotic form of the map P becomes P_{as} given by

$$q_{as}(n+1) = q_{as}(n) + p_{as}(n) \qquad p_{as}(n+1) = p_{as}(n)\,. \tag{9}$$

In the asymptotic region the momentum $p_{in/out}$ is conserved and can be used as one of the labels. To get the second one, we take an interval $Q(p_{in}) = (q_1, q_2)$ of q values where $q_2 = q_1 - p_{in}$ and choose q_1 independent of p_{in} and sufficiently large such that the whole interval lies well in the asymptotic region. Each asymptote with momentum p_{in} steps exactly once into $Q(p_{in})$ at the point $q_{in/out}$ and this particular value of q is used as the second label for the asymptote. To obtain the time-delay function $Dt(q_{in}; p_{in})$ fix some convenient choice of p_{in} (here convenient means that the interval $Q(p_{in})$ intersects the stable manifolds of the invariant set transversally), scan the interval $Q(p_{in})$ and plot Dt versus q_{in}—figure 4 shows the example for $A = 3.4$, $p_{in} = -4$. We have chosen $q_1 = 7$. Part (a) shows this function on its whole domain $Q(p_{in})$. In most parts it is not very interesting. Only the small part around $q_{in} = 10.05$ contains all the structure we are interested in. Part (b) gives a magnification of this interesting subinterval. We see a castle-like structure where each gap between two consecutive singularities is surrounded by smaller non-singular intervals with a higher value of Dt. This structure is continued *ad infinitum* in a fractal hierarchy. Part (c) gives a further magnification of a small part of figure 4(b) to show the self-similar structure of the whole function.

Several horizontal lines (labelled by level numbers m) separated vertically by a distance of 1 are included. The one with label m lies at the height $Dt_m = 4.5 + m$. These horizontal lines cut out intervals $J_i^{(m)}$ with the following properties: the boundary points of $J_i^{(m)}$ are infinities of Dt, inside of $J_i^{(m)}$ the value of Dt is always larger than Dt_m, and the values of Dt in the adjacent non-singular intervals outside of $J_i^{(m)}$ are smaller than Dt_m. A few of these intervals are indicated in the figures. Let the number of disjoint intervals $J_i^{(m)}$ on level m be $N(m)$. Then in the limit of large m we expect $N(m)$ to grow like $N(m) \propto \exp(mK_0)$, where K_0 is the topological entropy of the system. The value of $B = \exp(K_0)$ obtained by this method is the quantity plotted in figure 1 as function of the parameter A.

Next we have to correlate the structure in the time-delay function with the homoclinic tangle shown in figures 2 and 3, and in particular with the structure of the intersections of W^u with the local branch of W^s (i.e. the piece between x_0 and y_3 which is a part of the arc $L_{s,-}$). In particular, the hierarchical organisation of both structures is the same and should be described by the same symbolic dynamics. Figure 5 shows the corresponding branching tree. First let us explain how this branching tree taken together with its mirror image contains the castle-like structure of the time-delay function. On level -1 we cut out that part of $Q(p_{in})$ in which $Dt > 3.5$. This is the interval $J_1^{(-1)}$ and it contains the complete castle structure. At level 0 (i.e. in the height of the horizontal line at $Dt_0 = 4.5$) a first gap occurs which cuts away a middle piece of $J_1^{(-1)}$ and two connected subintervals $J_1^{(0)}$ and $J_2^{(0)}$ are created on level 0. To the right one (i.e. to $J_2^{(0)}$) the branching tree as shown in figure 5 applies and to the left one (i.e. to $J_1^{(0)}$) the mirror image of figure 5 applies. Going from level 0 to level 1 each of the two intervals of level 0 is cut into two pieces of level 1. To the two outer intervals we give the label 0, to the two inner ones we give the label 1. In the next step, the one from level 1 to level 2, the two outer intervals are cut, the two inner ones are not cut. Here and in the higher levels we construct labels by the following rules: if an interval of level m is not cut during the transition from level m to level $m+1$, then the resulting interval on level $m+1$ get its label by adding a + to the label

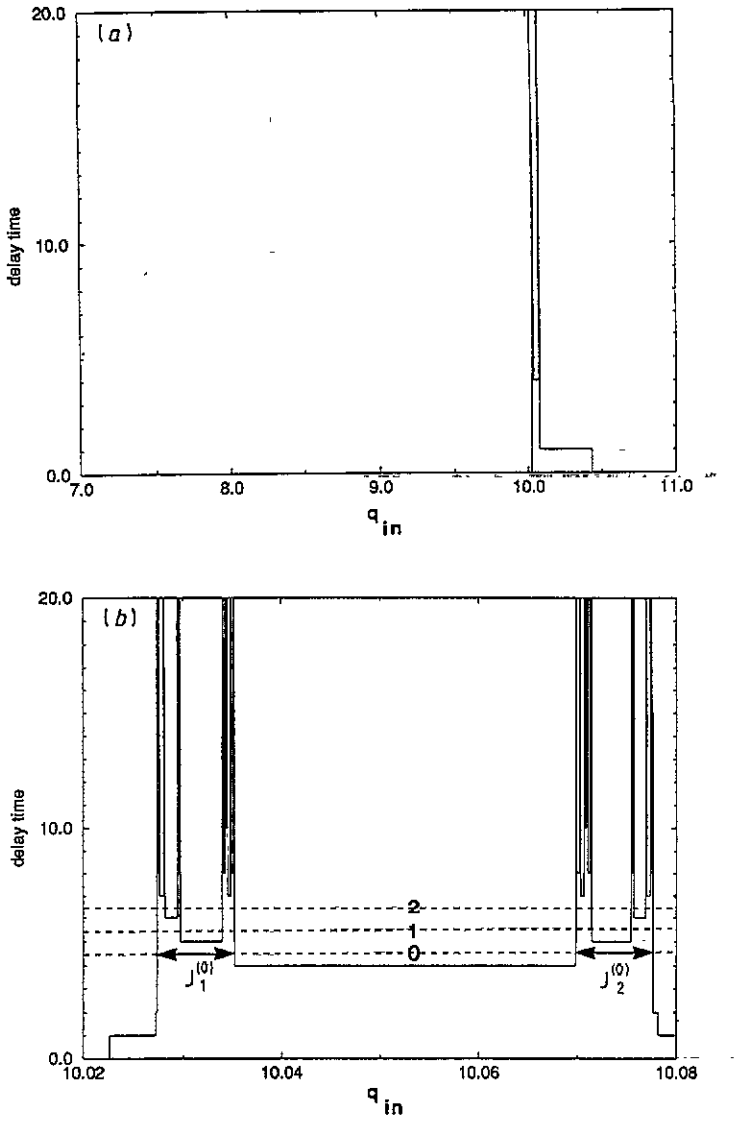

Figure 4. Plot of the time-delay function of system (1) for the parameter value $A = 3.4$ and initial conditions $p_{in} = -4$. Part (*a*) shows the function on its whole domain, i.e. for $q_{in} \in (7, 11)$, part (*b*) gives the magnification of the interesting part containing all singularities, part (*c*) shows a further magnification to demonstrate the self similarity. Several horizontal lines at heights $Dt_m = 4.5 + m$ are included and labelled by m. They indicate how the intervals $J_i^{(m)}$ are cut out. A few of these intervals are indicated and labelled in the figures.

of its parent interval of level m. If an interval of level m is cut into two pieces during the transition from level m to level $m + 1$ then the labels of the resulting two new intervals of level $m + 1$ are obtained by adding either a 0 or a 1 to the label of the parent interval. The rule for the distribution of the 0 and 1 is as follows in the right half of the castle (in the left half it is just the other way around): if in the label of the parent interval there is an even number of 1s then the new interval on the right side gets the 0 and the new interval on the left side the 1. For an odd number of 1's in the label of the parent interval it is the other

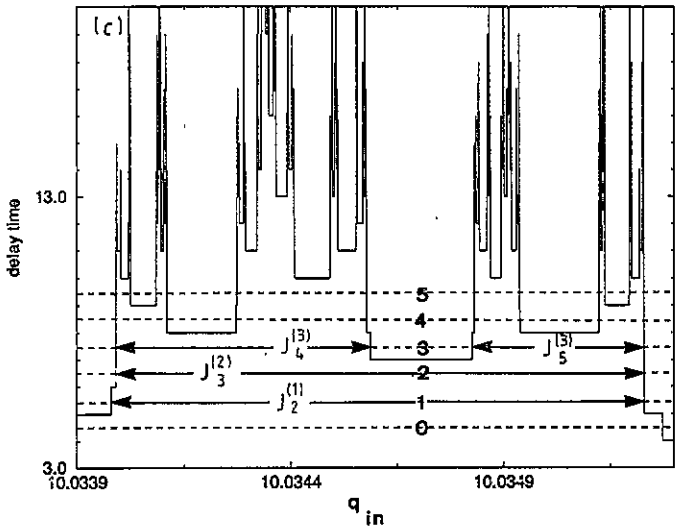

Figure 4. (Continued)

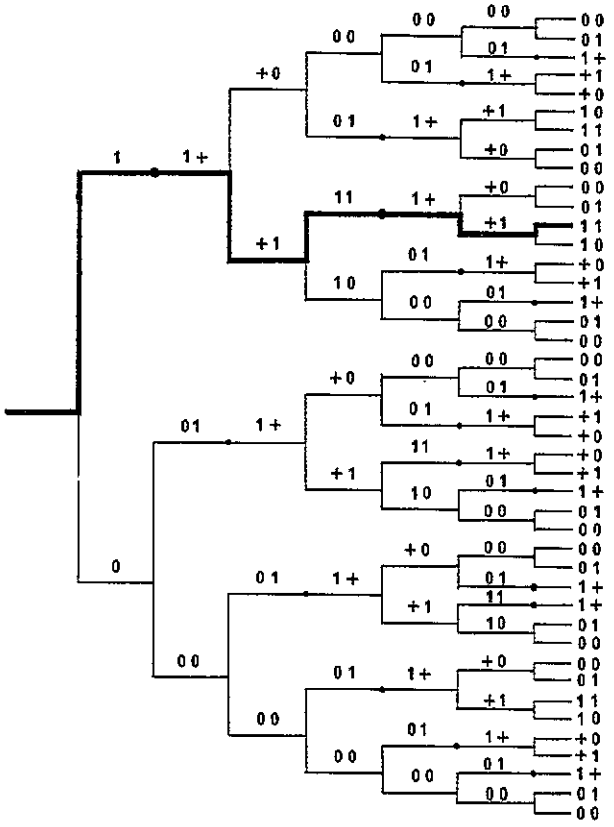

Figure 5. Branching tree for $A \in I_{1/2}$. The branch containing the longest intervals of each level is plotted by a thick line. Each entry is labelled by the last two digits of its symbolic code.

way around. This rule takes into account that the fixed point x_1 (which corresponds to the symbol 1) is inverse hyperbolic and the map inverts the orientation in its vicinity. These rules also go over into the standard symbolic dynamics of the horseshoe in the complete case. figure 5 shows the tree up to level 6 for the case of $\alpha = \frac{1}{2}$. Because only the last two digits of all labels are important for the following, we write only these last two digits in the figure.

Now let us compare this branching tree with the intersection structure between W^u and W^s along the interval $L_{u,-}$ as shown in figures 2 and 3. Regarding only tendrils up to hierarchy level 0 we obtain only the single interval $J_1^{(0)} = (x_0, y_3)$. Going next up to hierarchy level 1 the tendril of level 1 of W^s cuts a gap into the middle of $J_1^{(0)}$ leaving two subintervals, one from x_0 to y_4 which we call $J_2^{(1)}$, the other one from y_5 to y_3 which we call $J_1^{(1)}$. The interval $J_1^{(1)}$ is not cut any further by the tendril of level 2 of W^s and it coincides with the interval $J_1^{(2)}$ of level 2 whereas the interval $J_2^{(1)}$ is cut by $L_{s,2}$ into the two subintervals $J_2^{(2)}$ and $J_3^{(2)}$ of level 2. If we continue this scheme for higher levels then we repeat exactly the branching scheme of the delay function as presented in figure 5. Of course, for the intervals along $L_{s,-}$ we use the same symbolic codes again as for the intervals in the time-delay function. In this way the delay function reflects the structure created by the homoclinic tangle of the outermost hyperbolic fixed point. We can formulate the grammatical rules in the form that we say which symbols are allowed to be appended on an existing string. As we shall see the rules depend on the last two digits of the already present string. In the case that the present string has length 0 or 1 we can imagine that it is supplemented to the left by a string of 0's of arbitrary length.

The structure of the branching tree for $A \in I_{1/2}$ can be condensed into the following 5 rules:

- after symbol strings ending on 0 it is allowed to attach either 0 or 1
- after symbol strings ending on 01 it is only allowed to attach +
- after symbol strings ending on 11 it is only allowed to attach +
- after symbol strings ending on +1 it is allowed to attach either 0 or 1
- after symbol strings ending on 1+ it is allowed to attach either 0 or 1.

These rules lead to the following recursion relation for the number $Z(m, 1/2)$ of intervals which occur in the branching tree for $A \in I_{1/2}$ on level m:

$$Z\left(m, \frac{1}{2}\right) = Z\left(m-1, \frac{1}{2}\right) + 2Z\left(m-3, \frac{1}{2}\right). \tag{10}$$

To construct the transfer matrix $\mathbf{M}$ for the above rules, take the five end pieces e_i of symbol strings considered in the grammatical rules in the above order: $e_1 = 0$, $e_2 = 01$, $e_3 = 11$, $e_4 = +1$, $e_5 = 1+$. The matrix element $M_{i,j}$ has the value 1, if it is allowed to attach a symbol to a string ending on e_i in such a way that the new end becomes e_j. $M_{i,j}$ has the value 0 otherwise. We obtain

$$\mathbf{M}_{1/2} = \begin{pmatrix} 1 & 1 & 0 & 0 & 0 \\ 0 & 0 & 0 & 0 & 1 \\ 0 & 0 & 0 & 0 & 1 \\ 1 & 0 & 1 & 0 & 0 \\ 1 & 0 & 0 & 1 & 0 \end{pmatrix}. \tag{11}$$

The characteristic polynomial of $\mathbf{M}_{1/2}$ has the form

$$P_{1/2}(\nu) = \nu^2(\nu^3 - \nu^2 - 2). \tag{12}$$

Its non-trivial factor is consistent with the recurrence relation (10). The largest root of $P_{1/2}$ is $\nu = 1.71\ldots$ which coincides with the branching ratio B for $A \in I_{1/2}$ found in figure 1 which has been constructed directly from the time-delay function.

So far we have considered the invariant manifolds of the fixed point x_0 only. Fortunately, the invariant manifolds of all other unstable periodic points, which are accessible to scattering trajectories, show essentially the same behaviour. The accumulation points of homoclinic points of x_0 coincide with the accumulation points of homoclinic points of these other unstable periodic points and therefore with that part of the hyperbolic component of the invariant set which is accessible to scattering trajectories. Accordingly the absence of homoclinic bifurcations of x_0 in some open parameter interval indicates the absence of homoclinic bifurcations in the whole part of the invariant set which is relevant for the scattering behaviour. Furthermore, x_0 is the outermost periodic point, the one sitting on top of the potential barrier which divides the inside and outside regions of the position space. Therefore, the end points of non-singular intervals in the time-delay function are given by initial conditions which lie on the stable manifold of x_0. So the invariant manifolds of x_0 are the ones which determine the properties of the time-delay function and the other scattering functions.

4. Limitation of the symbolic dynamics

So far we have tried to construct a symbolic description with a finite number of rules for a non-hyperbolic system having an incomplete horseshoe. Of course, this construction can only be approximate, since the exact grammar for a symbolic dynamics of such a system should have an infinite number of rules. In this section we show briefly what we have not described correctly by the construction done above and what types of errors occur. This can be seen best in a more detailed figure of the tendrils as shown in figures 6 and 7. Figure 6 shows two magnifications of the numerical construction of the manifolds and figure 7 shows the corresponding schematic plots of the essential parts. In figure 6 the parameter value $A = 4.15$ has been chosen which still lies inside $I_{1/2}$ but very close to its upper end, where the errors in our approximate symbolic dynamics become visible even in quite low levels of the hierarchy. Therefore such parameter values are better suited to demonstrate the type of errors which occur. However, this type of error is always the same; only for parameter values not so close to the upper end of the interval they become noticeable, only in higher levels of the hierarchy. The important feature in figure 6(a) is: in a place where we expect just one transversal intersection between W^s and W^u there are really three intersections. This triple intersection is marked by three small circles in the figure. Figure 7(a) gives a schematic view of what we expect according to our symbolic dynamics and figure 7(b) shows in a schematic plot what we find instead, namely a triple intersection between W^s and W^u. In images and pre-images of these points under the map P this leads to secondary tendrils as the ones shown in figure 6(b) for the numerically constructed manifolds and shown in the schematic view in figure 7(c).

These secondary tendrils can create additional homoclinic intersections not contained in our symbolic dynamics. And under small changes of A the tips of these secondary tendrils can undergo homoclinic tangencies also in parameter intervals in which there are no homoclinic bifurcations created by the tips of the primary tendrils. The secondary structure shown in figure 6(a) is the one occuring on the lowest level of the hierarchy (level 5 in the case of $A = 4.15$) and at this level it is not yet noticable in the time-delay function. There it occurs for the first time at level 10, i.e. at the level at which the secondary tendrils

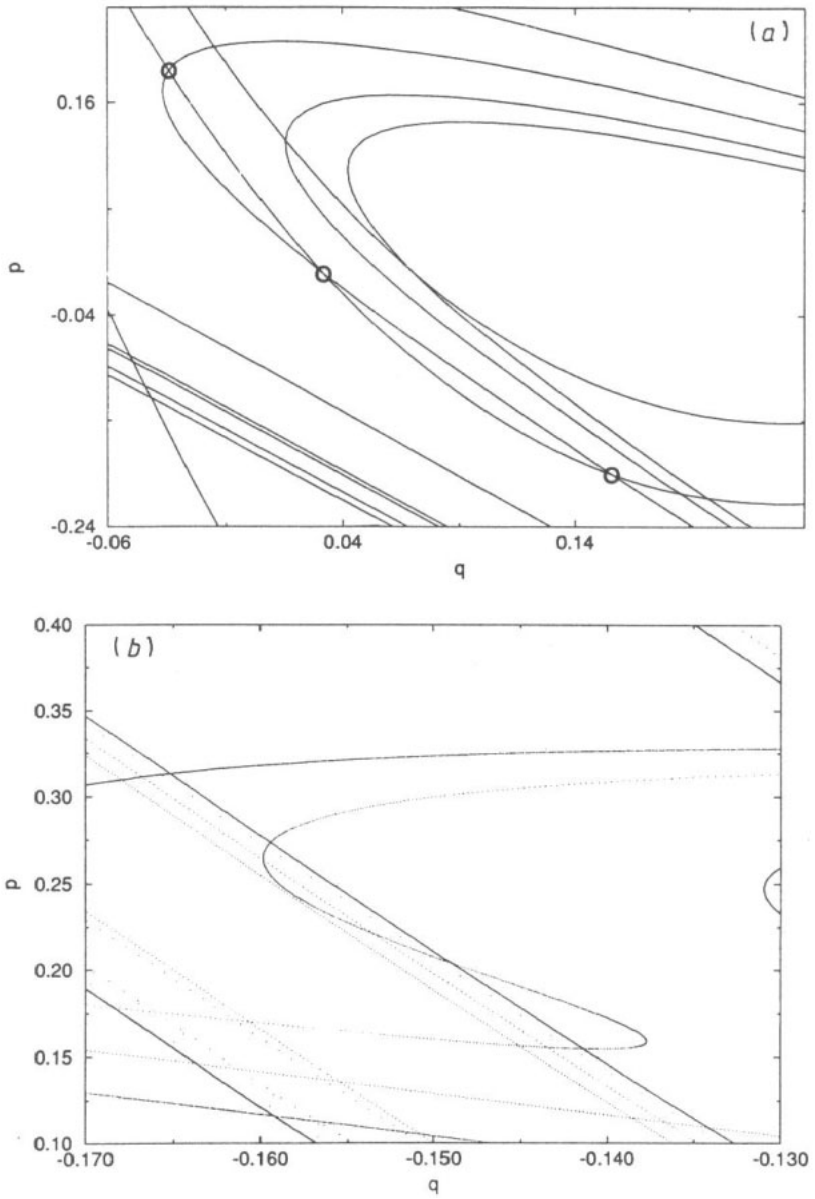

Figure 6. Small part of the homoclinic tangle of x_0 for the parameter value $A = 4.15$. In part (a) note the triple intersection, marked by circles, which is not contained in our approximate symbolic description. Part (b) shows an example of how the images and pre-images of triple intersections lead to secondary tendrils, whose intersections do not fit into the scheme of our approximate symbolic dynamics.

start to create homoclinic intersections along $L_{u,-}$. However, at higher levels the number of secondary structures increases rapidly and they dominate the behaviour of the system for $m \to \infty$. The structure of the tendrils must become more complicated for high levels, since there are KAM tori in the phase space. For sufficiently high levels the tendrils of W^u and

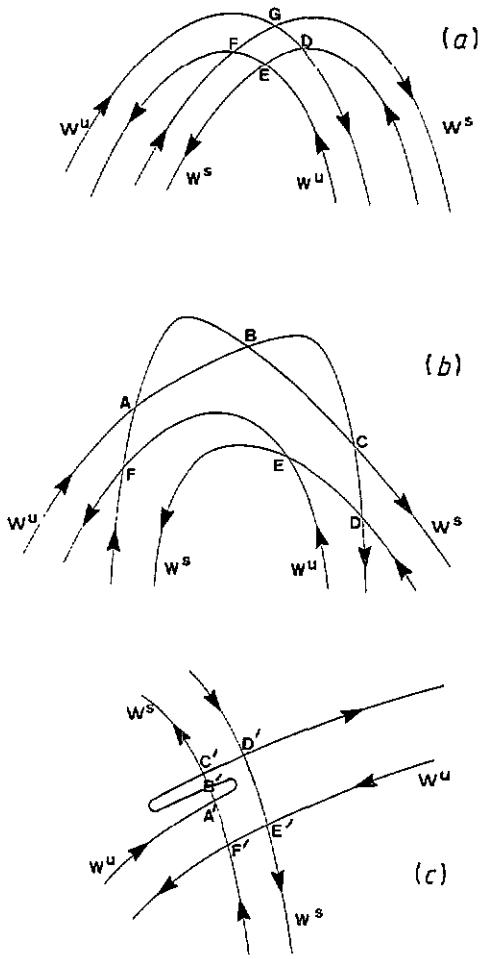

Figure 7. Schematic plots of small sections of the homoclinic tangle. Part (*a*) shows the structure we would have in the case that our symbolic dynamics is exact. Part (*b*) shows the actual structure we find instead of the one shown in part (*a*). Part (*c*) illustrates how images and pre-images of triple intersections lead to secondary tendrils. The points A′, B′, C′, D′ and E′, F′ in part (*c*) are the images or pre-images of the points A, B, C, D, E and F in part (*b*). In the transition from part (*a*) to part (*b*) the single intersection point G splits into the three intersection points A, B and C. The schematic plots of parts (*b*) and (*c*) correspond to the essential lines in the numerically constructed plots of figures 6(*a*) and 6(*b*).

W^s come close to the surface of the KAM tori and dive into the fractal jungle of Cantori and secondary structures around the KAM tori. Of course, our symbolic dynamics with a finite number of rules can never be able to describe complications of this type. It is only able to describe the hyperbolic component of the invariant set.

It is possible to invent a more complicated symbolic dynamics including the secondary tendrils for those parameter intervals in which their tips reach into some gap inside primary or secondary tendrils. However, this symbolic dynamics would not be exact because on higher levels these secondary tendrils also create more complicated intersection patterns leading to side tendrils of their own, which would not be included in the improved symbolic dynamics. Including them by a still improved symbolic dynamics would not describe the still more complicated intersection patterns on still higher levels etc. In the limit of arbitrarily high levels the exact symbolic dynamics would have to include an infinite set of levels of more complicated intersection patterns and would therefore require an infinite set of rules.

In this sense we are satisfied that our symbolic dynamics is only valid for low levels of the hierarchy and for small values of the delay time in the time delay function. As we shall see in the next section, for $A = 3.4$ our symbolic dynamics remains useful up to level 30 at least.

5. Thermodynamical formalism

As shown in [8, 11, 12] a very powerful method to extract characteristics of the invariant set from data obtained by asymptotic measurements is the so-called thermodynamical formalism. The procedure is the following: let $l_i^{(m)}$ be the length of the interval $J_i^{(m)}$ in the time-delay function as defined in section 3. Form the partition sum

$$Z(\beta, m) = \sum_i (l_i^{(m)})^\beta \sim \exp(-\beta F(\beta) m) \tag{13}$$

where β is a real parameter. The last proportionality becomes valid strictly only in the limit $m \to \infty$. However, as explained above, we are mainly interested in lower levels of the hierarchy and so we approximate $\beta F(\beta)$ as

$$\beta F_{l,m}(\beta) = [\ln(Z(\beta, m-l)) - \ln(Z(\beta, m))]/l\,. \tag{14}$$

Next we have to find a clever choice of l and have to see whether $\beta F_{l,m}(\beta)$ stabilizes as a function of m at least in some intermediate range of m values.

For complete horseshoes without any pruning (corresponding to a complete n-ary branching tree) it is known [8] that the choice $l = 1$ works well. As the region of large β is most sensitive to problems of convergence, let us do the following. Compute $\beta F_{l,m}(\beta)$ according to (14) for $l = 1$ and plot the asymptotic slope of this function versus m. The result for $A = 3.4$ can be seen in figure 8. For very small values of m (i.e. $m < 11$) there is no clear tendency visible. For larger values of m we see a periodicity with period 3 because of the following reason: for large β the sum is dominated by the interval of greatest length. When we climb up the branching tree along the branch containing the longest intervals of any level (this is the branch drawn by a thick line in figure 5, it has a periodic symbolic code with the basic block +11 repeated indefinitely) then we encounter symbols periodically with period 3 and also the ratio of the length of the intervals of consecutive levels changes periodically with period 3. This length ratio (i.e. $l_i^{(m+l)}/l_j^{(m)}$ along this path) determines the

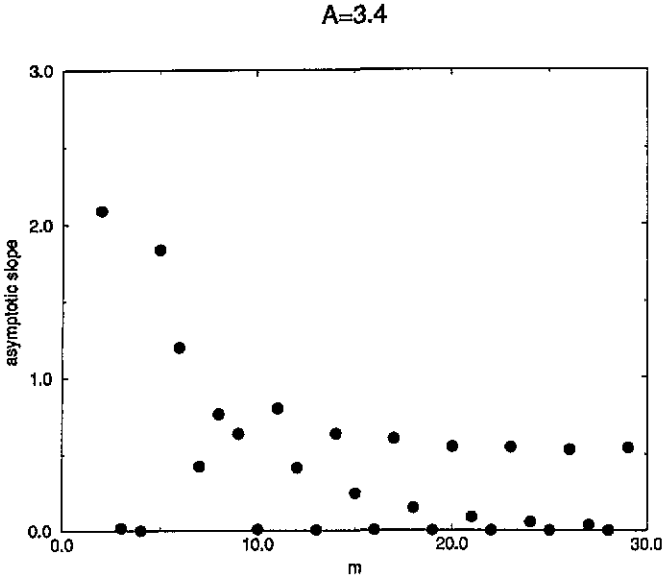

Figure 8. Asymptotic slope for $\beta \to \infty$ of the free energy function $\beta F_{l,m}(\beta)$ obtained from (14) with $l = 1$ versus the level m. The parameter $A = 3.4 \in I_{1/2}$.

asymptotic slope of $\beta F_{l,m}(\beta)$ for $\beta \to \infty$. Climbing up the branching tree by three steps along this path leads to the same local situation and therefore also to the same length ratio regardless of the value of m. Therefore, $l = 3$ is the appropriate choice for the evaluation of (14) for $A \in I_{1/2}$. For very large values of m the periodicity fades out (for $A = 3.4$ we did not reach this region in our numerical computations). Then the non-hyperbolic effects not contained in our approximate symbolic description start to dominate the behaviour of the system—the branching tree of figure 5 becomes invalid, there are further divisions of intervals and the position of the longest interval starts to jump in an unpredictable way between various branches from level to level.

We do not encounter convergence problems for small values of β since this convergence behaviour is directed by the shortest intervals. They are always the intervals whose symbolic code consists of 0s only. This sequence always has a period 1 and therefore always fits together with any other period occuring in the range of large β values.

The value m_{nh} of m at which non-hyperbolic effects start to dominate depends on the exact value of A. As an inspection of figure 1 shows, the value of B increases monotonically with increasing A inside the interval $I_{1/2}$. This indicates that m_{nh} is quite small near the upper end of $I_{1/2}$, in fact it is so small that the region of periodic behaviour of the slope of $\beta F_{1,m}(\beta)$ as shown in figure 8 does not exist at all for these values of A.

Next we choose a value of m well inside the range of periodic behaviour of figure 8, namely $m = 17$, and plot the resulting function, $\beta F_{3,17}(\beta)$ computed according to (14) with $l = 3$ and $m = 17$ versus β, in figure 9 as a full curve. This plot provides the following characteristics of the hyperbolic component of the invariant set [8]: the topological entropy is $K_0 = -\beta F(\beta)$ at $\beta = 0$, the fractal dimension D_0 is the value of β at which $\beta F(\beta) = 0$, the escape rate $\kappa = F(1)$ and the Lyapunov exponent λ is the slope of this function at

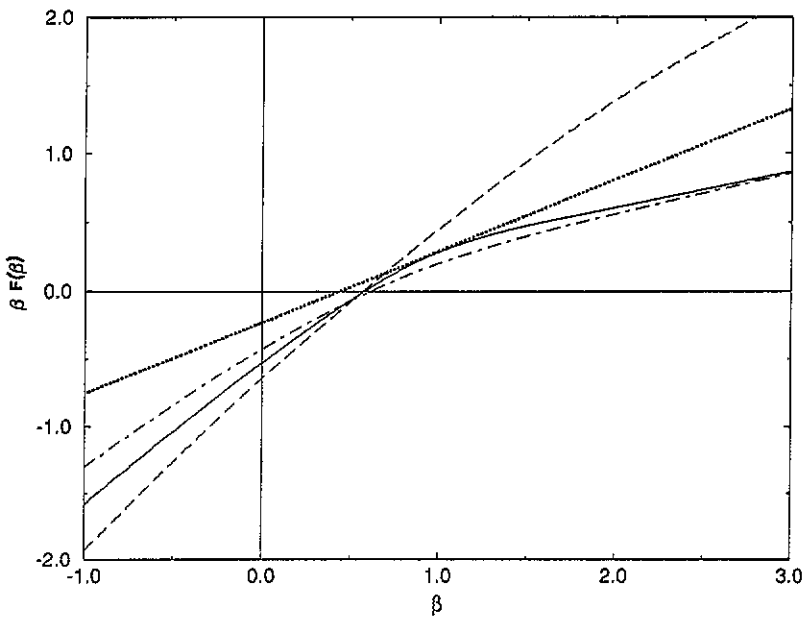

Figure 9. Plot of $\beta F_{l,m}(\beta)$ versus β computed according to (14). The full curve is for $m = 17$, $l = 3$ and $A = 3.4 \in I_{1/2}$ as in figure 8. The broken curve is for $m = 17$, $l = 5$ and $A = 4.96 \in I_{3/4}$ and the chain curve is for $m = 17$, $l = 4$ and $A = 2.4 \in I_{1/4}$. The dotted line is the tangent to the solid line at $\beta = 1$.

$\beta = 1$. The tangent to the curve at $\beta = 1$ (the dotted line in figure 9) intersects the β-axis at the value of the information dimension D_1 and the vertical axis at minus the value of the metric entropy K_1. We read off the following numerical values: $K_0 = 0.54$, $D_0 = 0.57$, $\kappa = 0.26$, $\lambda = 0.48$, $D_1 = 0.46$, $K_1 = 0.22$. Of course, these values only characterize the short-time properties of the systems, strictly speaking they apply to the time scale between 14 and 17. For long times the non-hyperbolic effects take over and it is known [22, 23] that in this case $\lambda = \kappa = 0$, $D_0 = 1$ expressing the stickiness of the fractal surface of KAM tori. These values correspond to the fact that for non-hyperbolic systems the true free energy function computed according to (13) in the limit $m \to \infty$ (expressing the long-time behaviour of the system) becomes identically zero for $\beta > 1$. For comparison the broken curve and the chain curve in figure 9 give $\beta F_{5,17}(\beta)$ for $A = 4.96 \in I_{3/4}$ and $\beta F_{4,17}(\beta)$ for $A = 2.4 \in I_{1/4}$ respectively.

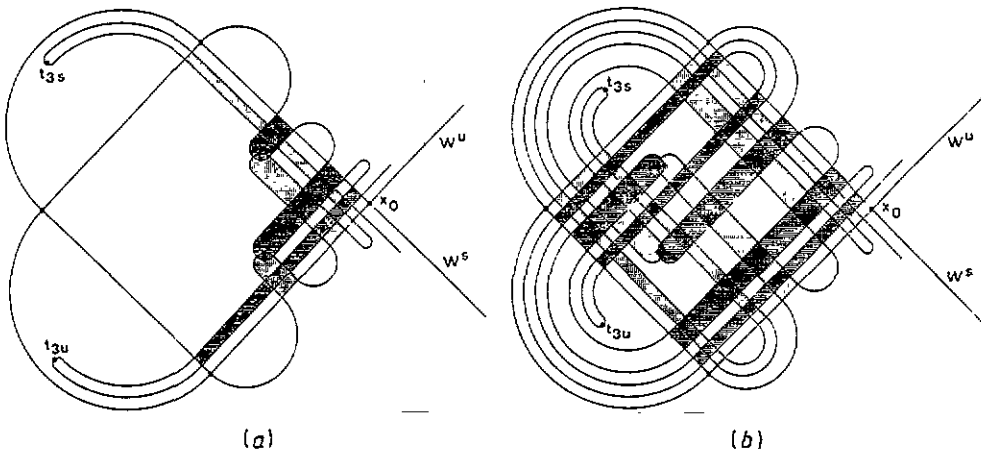

Figure 10. Schematic plot of the homoclinic tangle of x_0 for $\alpha = \frac{1}{4}$ in part (a) and $\alpha = \frac{3}{4}$ in part (b). Tendrils up to level 3 are included.

6. Different intervals I_α

So far we have considered the particular parameter interval $I_{1/2}$ only. In figure 1 there are many more intervals of slow variation of $\exp(K_0)$ and next let us explain how we can give an approximate symbolic dynamics for these other intervals. Because the homoclinic grid for the complete horseshoe as shown in figure 3(d) has a binary organisation, it is useful to construct the parameter α in an adapted binary way as explained above.

The next simple cases to be investigated are the cases $\alpha = \frac{1}{4}$ and $\alpha = \frac{3}{4}$. The schematic plot of the tendrils for $\alpha = \frac{1}{4}$ is given in figure 10(a). The corresponding branching tree is shown in figure 11. The periodicity along the branch of the longest intervals (the thick line in the figure corresponding to a periodic symbolic code with basic block 11++ repeated indefinitely) is four. Therefore we need $l = 4$ in this case for the evaluation of the thermodynamics according to (14) (see the chain curve in figure 9). Each entry of the branching tree is labelled by the last two digits of its symbolic code. The grammatical rules for $\alpha = \frac{1}{4}$ are:

- after symbol strings ending on 0 or +1 or ++ it is allowed to attach 0 or 1
- after symbol strings ending on 01 or 11 or 1+ it is only allowed to attach +.

The characteristic polynomial of the corresponding transition matrix is

$$P_{1/4}(\nu) = \nu^2(\nu^4 - \nu^3 - 2) \tag{15}$$

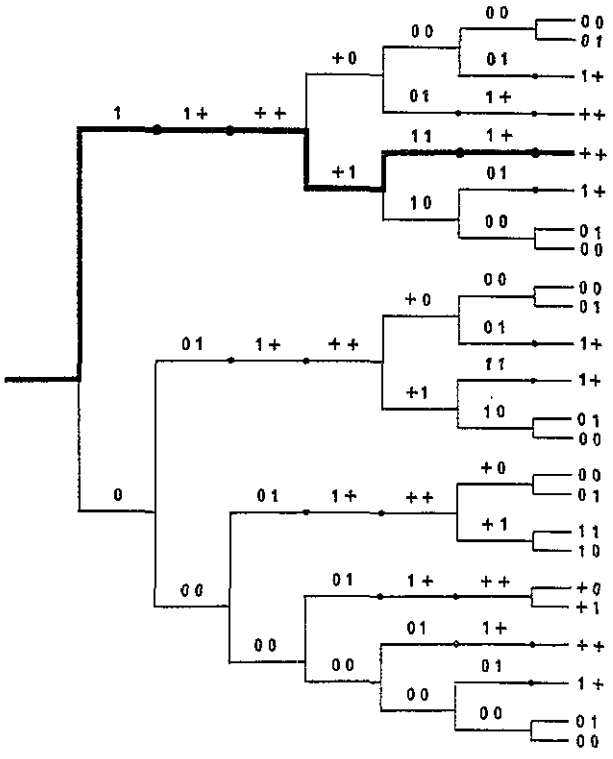

Figure 11. Branching tree for $\alpha = \frac{1}{4}$. The branch containing the longest interval of each level is plotted by a thick line. Each entry is labelled by the last two digits of its symbolic code.

and the corresponding recurrence relation for the number of intervals on level m is

$$Z\left(m, \tfrac{1}{4}\right) = Z\left(m-1, \tfrac{1}{4}\right) + 2Z\left(m-4, \tfrac{1}{4}\right). \tag{16}$$

The largest root of $P_{1/4}$ is $\nu = 1.54\ldots$ which coincides with the value of B found numerically in figure 1 for the corresponding step around $A = 2.5$.

More generally, for any $\alpha = 2^{-k}$ the symbol + always comes in blocks of length k only, such a string begins after 01 and is followed by either 0 or 1. The non-trivial factor of the characteristic polynomial is

$$P_{2^{-k}}(\nu) = \nu^{k+2} - \nu^{k+1} - 2 \tag{17}$$

where the complete polynomial contains an additional factor consisting of a pure power of ν. The corresponding recurrence relation for the number of intervals on level m is

$$Z(m, 2^{-k}) = Z(m-1, 2^{-k}) + 2Z(m-2-k, 2^{-k}). \tag{18}$$

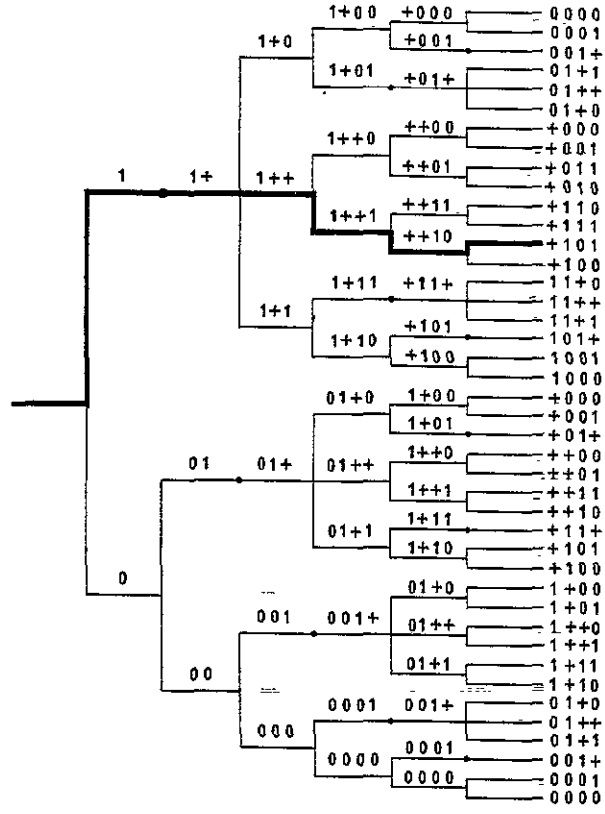

Figure 12. Branching tree for $\alpha = \frac{3}{4}$. The branch containing the longest interval of each level is plotted by a thick line. Each entry is labelled by the last four digits of its symbolic code.

These rules are also valid for $k = 0$ in which case they describe correctly the complete case for $A > A_1$.

Things become a little more complicated if in $\alpha = r2^{-k}$ we have $r \neq 1$. Then it sometimes happens that an interval is cut into three subintervals during the transition from one level to the next level. In such a case we append the symbol + to the label of the middle subinterval. Let us look closer at the case $\alpha = \frac{3}{4}$: the schematic plot of the homoclinic grid is given in figure 10(*b*) and the branching tree obtained from either the time-delay function or the homoclinic grid is given in figure 12. Again the branch containing the longest intervals of each level is plotted by a thick line, it corresponds to a periodic symbolic code with basic block 101++ repeated indefinitely. The period for the convergence of the thermodynamics following from it is $l = 5$ (see the dashed line in figure 9). Now the grammatical rules are more complicated, we need to know the last four digits of the symbolic code of each entry to decide how the tree is continued. For the lowest levels of the tree we can imagine again, that each symbolic code is supplemented to the left by a string of 0's of arbitrary length. The grammatical rules are:

- after symbol strings ending on 0 or ++ or ++01 or ++11 or 111 or 011 or +1 it is allowed to attach 0 or 1
- after symbol strings ending on 1+ it is allowed to attach 0 or 1 or +
- after symbol strings ending on 001 or 101 or 1+01 or 1+11 it is only allowed to attach +.

The corresponding non-trivial factor in the characteristic polynomial of the transition matrix is

$$P_{3/4}(\nu) = \nu^5 - 2\nu^4 + \nu^3 - 2\nu^2 + 2\nu - 2\,. \tag{19}$$

Its largest root is close to $\nu = 1.9$ coinciding with the numerical value of B extracted from figure 1 for A around $A = 4.9$.

When we try to treat all values of α along similar lines, we must notice two additional complications: first, not all values of $\alpha = r2^{-k}$ really lead to cases for which the tendrils of W^u and W^s reach into empty gaps. Let us illustrate this phenomenon for the case $\alpha = \frac{3}{8}$. Starting from the schematic plot of the complete homoclinic tangle shown in figure 3(*d*) we would expect that the case $\alpha = 3/8$ occurs when the tip of the tendril of level 1 has shrunk such that it reaches into the gap created by the tendril of level 3 and the tips of the tendrils of level 2 reach into the gaps created by the other tendrils of level 2. In the schematic plot in figure 13 we have plotted by broken lines the gaps created by W^u up to level 3 in the complete case. The label 3 indicates that particular gap of level 3 into which we expect the tip of the tendril of level 1 of W^s to reach. Similarly, the label 2 indicates that particular gap of level 2 into which we expect the tip of the tendril of level 2 of W^s to reach. The actual tendrils of levels 2 and 3 of W^s are also plotted. Now the problem becomes evident: for $A \in I_{3/8}$ the tendrils of W^u have already withdrawn from this part of the phase space so that the gaps do no longer exist. Therefore, the interval $I_{3/8}$ does not exist and in figure 1 we do not find any nearly horizontal step corresponding to $\alpha = \frac{3}{8}$.

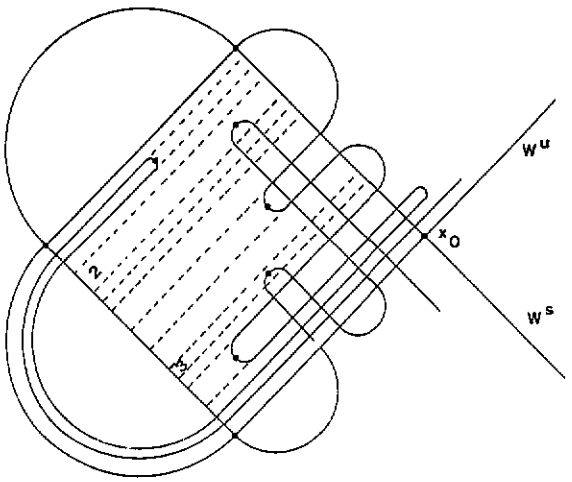

Figure 13. The solid line gives a schematic view of the homoclinic tangle in a parameter range in which we would expect the interval $I_{3/8}$ to exist. The broken line shows the gaps created by W^u as they appear in the complete horseshoe shown in figure 3(*d*). The labels 2 and 3 mark a gap of level 2 and a gap of level 3 which have already disappeared for the actual value of the parameter.

The second difficulty can be explained best for the example of $\alpha = \frac{7}{8}$. Let us first, in figure 14, give a schematic view of a small section of the homoclinic grid for three different values of A. We plot short segments of gaps of levels 2, 4, 5 created by W^s intersecting

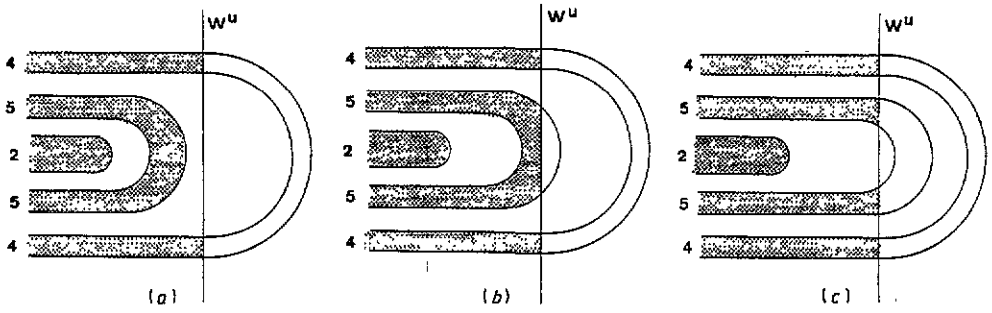

Figure 14. Schematic view of a small section of the homoclinic tangle for A below, inside and above the interval $I_{7/8}$ in parts (a,b,c) respectively. Some segments of the tendrils of W^s are shown and labelled by their level numbers. The interior of the tendrils of W^s is dotted in that part which lies inside of R. From W^u only the arc $L_{u,-}$ is shown and labelled by W^u.

the local branch of W^u. The tendril of W^s of level 3 has already withdrawn so that we do not find intersections of it with W^u_- in this region. Now we have to decide which of these three situations is the appropriate one for $\alpha = \frac{7}{8}$. We choose the situation shown in figure 14(b) for the following reason. In situation (a) the fate of tendrils of W^s of higher levels is not yet determined. Tendrils running between the ones of level 4 and 5 shown in the figure either intersect W^u or can not, depending on the value of A. Similarly, for case (c) the fate of higher level tendrils running between the tendrils of levels 2 and 5 is not yet clear and changes under variations of A. On the other hand, we have decided to choose the intervals I_α such that for variations of A within I_α no homoclinic tangencies of primary tendrils are allowed to occur. Therefore only the range of A values for which a situation of the qualitative structure of figure 14(b) occurs can belong to I_α. In this case all higher level tendrils running between those of levels 2 and 5 do not intersect W^u in the region shown and all tendrils running between those of levels 4 and 5 intersect W^u twice. Only in case (b) is the intersection structure of higher level tendrils clearly determined and independent of small changes of A within I_α. For $I_{7/8}$ chosen this way it is straight foreward to obtain the branching tree and to construct from it the following set of grammatical rules for the approximate symbolic dynamics:

- after symbol strings ending on 0 or ++001 or 1101 or ++101 or 0101 or ++01 or 11 or +1 or +++ it is allowed to append 0 or 1
- after symbol strings ending on 0001 or 1001 or 1+001 or 1+101 or 1+01 it is only allowed to append +
- after symbol strings ending on 1++ or 1+ it is allowed to append 0, 1 or +.

The interval $I_{7/8}$ can be seen quite clearly in figure 1 at a height of $B = 1.97$ around the parameter value $A = 5.3$. So far we do not yet know, in which other intervals difficulties occur corresponding to the ones just explained for $I_{7/8}$.

To complete all cases of $k = 3$, we finally give the grammatical rules for $\alpha = 5/8$:

- after symbol strings ending on 0 or +1 or +++ it is allowed to append 0 or 1
- after symbol strings ending on 01 or 11 or 1++ it is only allowed to append +
- after symbol strings ending on 1+ it is allowed to append 0 or 1 or +.

The corresponding non-trivial factor in the characteristic polynomial is

$$P_{5/8}(\nu) = \nu^5 - \nu^4 - 2\nu^2 - 2\,. \tag{20}$$

Its largest root is close to $v = 1.8$. The interval $I_{5/8}$ is very small and hard to identify in figure 1.

Generally, we noticed that for $\alpha = r2^{-k}$ the symbol + can occur in blocks of maximal length k. And the branch in the branching tree which contains the longest intervals is the one which contains these blocks of +s in the maximally allowed density. The symbol + always corresponds to the largest ratio of the length of the intervals of two consecutive levels. There is never a fixed point in the system corresponding to the symbol +. Accordingly, an unlimited string of only +s never occurs. An unlimited string of 1s corresponds to the fixed point x_1 and this string is only allowed as long as the fixed point x_1 is accessible to scattering trajectories. The point x_1 becomes elliptic for $A < 4$ only, however, for $A < 4.7\ldots$ it is already screened behind some KAM lines and scattering trajectories can not come into its vicinity. Accordingly unlimited strings of 1s do not occur in the symbolic dynamics of the branching tree for the time-delay function for $A < 4.7\ldots$ and they are not allowed in the grammatical rules for $\alpha = \frac{5}{8}$ which belongs to a value of A just below 4.7. On the other hand, unlimited strings of 1s are allowed by the grammatical rules for α values corresponding to $A > 4.7\ldots$. See e.g. the grammatical rules for $\alpha = \frac{3}{4}$ or $\alpha = \frac{7}{8}$. After 0 it is always allowed to attach either 0 or 1 independently of the value of α. Accordingly the unlimited string of only 0s is always allowed. This is caused by the accessibility of the unstable fixed point x_0 to scattering trajectories for all values of A.

For all values of α there are analogous restrictions for the validity of the approximate symbolic dynamics like the ones we have described in section 4 for $\alpha = \frac{1}{2}$.

7. Discussion

For a particular model system having a non-hyperbolic invariant set in the form of an incomplete horseshoe we have constructed an approximate symbolic dynamics valid in some parameter intervals. The essential basic observation, which allowed this construction to be done, was that there are parameter intervals in which the tips of the primary tendrils of the invariant manifolds do not create homoclinic bifurcations under small changes of the parameter. This occurs due to the gaps which are empty of invariant manifolds. It only can happen in an open system describing scattering dynamics. In a closed Hamiltonian system the invariant manifolds are dense in a connected subset of the phase space not containing KAM tori. Therefore our ideas can only be applied to scattering systems or to systems with transient chaos.

The symbolic dynamics constructed is only approximate and describes the hyperbolic component of the invariant set. This is quite acceptable for scattering systems which are rather open because of the following: a real scattering experiment is done with many particles where initial conditions are evenly distributed over a wide range. Most particles run on trajectories which stay in the interaction region for a short time only. They come in contact with the hyperbolic component of the invariant set only. They do not have the necessary time to dive into the non-hyperbolic regions of the phase space sitting on the surface of KAM tori. Only very few trajectories (i.e. only a tiny fraction of all initial conditions) allow the particles to come sufficiently close to the KAM tori to be influenced essentially by non-hyperbolic effects. In this sense a good description of the hyperbolic component allows one to understand most properties of the scattering behaviour to a good approximation. This argument may fail for systems with tiny leaks only.

We have one particular symbolic dynamics for each of the parameter intervals $I_{r2^{-k}}$ defined in section 6. Of course, for large k these intervals become very short so that it will

be difficult to identify them. To do this we have to find values of A for which the tips of the high level tendrils (they change rapidly under variation of A) reach into the small gaps created by other tendrils of high levels. At the moment we do not know whether these intervals are dense on the whole parameter axis or whether there are open intervals on the A-axis in which homoclinic tangencies of the primary tendrils are dense under variation of A.

So far our considerations have been presented for an iterated map. How can something similar be done for systems with continuous time? For such systems it is difficult to get the branching tree from the sole knowledge of the time-delay function. For time continuous systems the minimal value of Dt within some interval of continuity is not an integer multiple of some basic time unit and therefore it is not clear how we obtain the hierarchical organisation of the intervals without further knowledge. However, we need this organisation to select all intervals of a particular level which we need as input for the thermodynamical formalism. Here the knowledge of an approximate symbolic dynamics can be of paramount importance because it allows the construction of a branching tree which tells us how to divide the intervals into the various levels of hierarchy. With the aid of the ideas presented in this paper such an approximate symbolic dynamics can be obtained from the homoclinic tangle of an appropriate periodic orbit in a Poincaré section of the system. The appropriate point is usually the fixed point corresponding to the outermost periodic orbit sitting on top of the barrier of the potential which divides the position space into the inside and the outside region. For these particular periodic orbits considerations are valid which are analogs of the statements about the fixed point x_0 given at the end of section 3. Instead of a Poincaré return map we can also use a stroboscopic map of a time continuous system as well. This possibility may order things differently, but is not any worse in principle.

As shown in [24] the knowledge of a symbolic dynamics is helpful to organize the summation of the semi-classical sum for the quantum scattering amplitude and to check for its absolute convergence. Of course, the symbolic dynamics is irrelevant to the questions whether the sum converges or not.

Acknowledgment

This work has been supported financially by the Deutsche Forschungsgemeinschaft.

References

[1] Eckhardt B 1988 *Physica* **33D** 89
[2] Smilansky U 1992 *Proc. 1989 Les Houches Summer School* ed M J Giannoni, A Voros and J Zinn-Justin (Amsterdam: North-Holland) pp 371–441
[3] Brumer P and Shapiro M 1988 *Adv. Chem. Phys.* **70** 365
[4] Petit J M and Henon M 1986 *Icarus* **66** 536
[5] Eckhardt B and Aref H 1988 *Phil. Trans. R. Soc.* A **326** 655
[6] Campbell D K, Peyrard M and Sodano P 1986 *Physica* **19D** 165
[7] Jung C and Ziemniak E 1992 *J. Phys. A: Math. Gen.* **25** 3929
[8] Tel T 1990 *Directions in Chaos* ed Bai-lin Hao vol 3 (Singapore: World Scientific) pp 149–221
[9] Jung C and Richter P 1990 *J. Phys. A: Math. Gen.* **23** 2847
[10] Smale S 1967 *Bull. Am. Math. Soc.* **73** 747
[11] Tel T 1989 *J. Phys. A: Math. Gen.* **22** L691
[12] Kovacs Z and Tel T 1990 *Phys. Rev. Lett.* **64** 1617
[13] Karney C F 1983 *Physica* **8D** 360
[14] Meiss J D and Ott E 1985 *Phys. Rev. Lett.* **55** 2741

[15] Ding M, Bountis T and Ott E 1990 *Phys. Lett.* **151A** 395
[16] Vollmer J and Breymann W 1993 *Helv. Phys. Acta* **66** 91
[17] Troll G 1991 *Physica* **50D** 276
[18] Troll G 1992 *Nonlinearity* **5** 1151
[19] Cvitanovic P, Gunaratne G and Procaccia I 1988 *Phys. Rev.* A **38** 1503
[20] Auerbach D and Procaccia I 1990 *Phys. Rev.* A **41** 6602
[21] Guckenheimer J and Holmes P 1983 *Nonlinear Oscillations, Dynamical Systems, and Bifurcations of Vector Fields* (New York: Springer) section 6.7
[22] Lau Y T, Finn J M and Ott E 1991 *Phys. Rev. Lett.* **66** 978
[23] Breymann W, Kovacs Z and Tel T 1993 *Preprint* Chaotic scattering in external fields
[24] Jung C and Pott S 1990 *J. Phys. A: Math. Gen.* **23** 3729